Accepted Manuscript

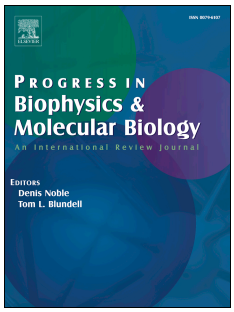

Stereochemical study of mouse muscone receptor MOR215-1 and vibrational theory based on statistical physics formalism

Ismahene Ben Khemis, Nesrine Mechi, Abdelmottaleb Ben Lamine

PII: S0079-6107(17)30241-9

DOI: 10.1016/j.pbiomolbio.2018.02.004

Reference: JPBM 1320

To appear in: *Progress in Biophysics and Molecular Biology*

Received Date: 15 November 2017

Revised Date: 2 February 2018

Accepted Date: 9 February 2018

Please cite this article as: Ben Khemis, I., Mechi, N., Ben Lamine, A., Stereochemical study of mouse muscone receptor MOR215-1 and vibrational theory based on statistical physics formalism, *Progress in Biophysics and Molecular Biology* (2018), doi: 10.1016/j.pbiomolbio.2018.02.004.

Stereochemical study of mouse muscone receptor MOR215-1 and vibrational theory based on statistical physics formalism

Ismahene Ben Khemis*, Nesrine Mechi and Abdelmottaleb Ben Lamine

Laboratory of Quantum Physics UR 11 ES 54, Faculty of sciences of Monastir, Environnement Street, 5019, Monastir, Tunisia.

Corresponding authors:

* Ismahene Ben Khemis, E-mail: ismaheneph@gmail.com.

Tel: +216 58 013 096.

Abstract

In the biosensor system, olfactory receptor sites could be activated by odorant molecules and then the biological interactions are converted into electrical signals by a signal transduction cascade that leads the toopening of ion channels, generating a current that leads into the cilia and depolarizes the membrane.

The aim of this paper is to present a new investigation that allows determining the olfactory band using a monolayer adsorption with identical sites modeling which may also describe the static and the dynamic sensitivities through the expression of the olfactory response. Moreover, knowing the size of receptor site in olfactory sensory neurons provides valuable information about the relationship between molecular structure and biological activity. The determination of microreceptors and mesoreceptors is mostly carried out via physical adsorption and the radius is calculated using the Kelvin equation. The mean values of radius obtained from the maximum of the receptor size distributions peaks are 4 nm for ℓ-muscone and 6 nm for d-muscone.

Keywords: transduction, adsorption model, olfactory response, sensitivity, olfactory band.

1. Introduction

The five senses, hearing, vision, touch, taste, and smell were first defined by Aristotle as the constituents of a living being's perceptivity. All sensory systems detect stimuli via specific sensory cells and receptors.

Photoreceptor cells of the eye undergo ion current changes upon photon detection by light sensitive cells. To understand the first steps of the visual transduction mechanism, it is necessary to investigate the interaction between the light and the photoreceptors which are illuminated with very low light intensities. Hecht, Shlaer and Pirenne in 1942 determined that the eye's detection limit corresponds to energies, incident at the cornea, in the range 2–6 10^{-17}

J, equivalent to 54–148 photons. To calculate the energy actually absorbed by the retinal receptors, they applied corrections to take account of absorption by the ocular medium (50%) and losses due to reflection (4% at the cornea). Likewise, at least 80% of the light is falling on the retina passes through unabsorbed. After all these corrections, they estimated that the number of photons absorbed by the visual pigment was in the range 5–14 [1].

The photoreceptor cells of the retina contains rod cells, which respond to weak light over a range of wavelengths, and three classes of cone cells, which respond to colors in bright light. Rhodopsin is the photoreceptor in rods and cones that occurs in four forms; each comprises one of four homologous opsin proteins (bathorhodospin, lumirhodopsin, metarhodopsin-I andmetarhodopsin-II)linked to 11-*cis*-retinal [2, 3, 4]. The principal enzymes of the transducing cascade are the G protein transducin (G_t) that transduces the light signal and the effector enzyme cyclic GMP phosphodiesterase. In the dark, the cation channels are held in their open configuration by the presence of cGMP. The effect of light is to initiate a series of molecular rearrangements in rhodopsin (There are effectively 10–20 molecules of cGMP for each molecule of rhodopsin) that generate activated rhodopsin (Rh*). This catalyses the exchange of GTP for GDP on transducin. The mechanism of phototransduction in cones is very similar to that of rods, differing only in terms of color specificity

Olfactory recognition and spatial functions appear to graft onto these anatomical pathways, described above for the visual system. However, distinctions between the olfactory and visual systems should be noted.

The mammalian olfactory system is capable of sensing and distinguishing several hundred different odorant molecules. All of these compounds are volatile molecules or a set of molecules, none has a molecular weight much greater than 300 Da and all have the ability to partition between lipid and aqueous phases [5].

As with the mechanism of phototransduction [6], the olfactory process allows enormous amplification of the initial signal. Olfaction in the mammalian olfactory epithelium is mediated by a large family of Guanine nucleotide protein (G protein)-coupled receptors (GPCRs) from the rhodopsin-related receptor superfamily. These are known collectively as odorant receptors. The total number of odorant receptor genes varies widely across species; mouse have about 900 functional odorant receptor genes (and ~1200 chemoreceptor genes in all), whereas humans have about 350 functional odorant receptor genes and have lost the vomeronasal (olfactory sense organ in most animals) receptors during evolution. These differences result both from duplication of genes in the mouse lineage and from extensive loss of genes in the human lineage [7].

The exploration of the olfactory sensory system of mammals is an appropriate model to study the fundamentals of the chemosensitivity and to understand the olfactory system. The olfactory system has the capacity to detect thousands or even hundreds of thousands of volatile molecules at very low concentrations and discriminate between them even differing by only one or few atoms [8]. In mammals, the odor molecules pass through the nasal cavity and move in the mucus [9]. So, hydrophobic odorants must cross an aqueous fluid which contains great concentration of odorant binding proteins (OBPs) that transport them to reach the olfactory receptors. Then, the odorant molecules adsorption on the olfactory receptor sites is a decisive step in the olfaction mechanism.

The present work purpose is to study the transformation of olfactory signals, to review how the olfactory response of the projection neurons depends on the odorant concentration and to drive the coding of this response in terms of its sensitivity. This study leads us to analyze the static and the dynamic sensitivity through the application of the statistical physics formalism which can give a physical significance of parameters introduced in biological disciplines such as the olfactory perception via muscone enantiomers adsorption onto the mouse muscone

receptor MOR215-1 [10], to determine the receptor site size distribution function thanks to the statistical physics formalism by the derivation of the olfactory response expression using the monolayer model with identical sites relative to receptor site radius and to define the olfactory vibrational frequencies band by applying the grand canonical formalism through the determination of the molar adsorption energies [11, 12].

2. Olfactory transduction

The olfactory transduction takes place in the cilia of olfactory receptor neurons that are essential to convert external chemical stimuli into intracellular electrical responses. The olfactory cilium is a nanotube structure with a very small volume (fL: femtolitre) [13] and embedded in a mucus layer [14]. The odorant molecules diffuse through the mucus in the olfactory epithelium and bind to small globular odorant binding proteins (OBPs) before reaching the odorant receptor sites. This idea is based on the expression of several OBPs in the same species, with different and complementary spectra of binding. Apparently, OBPs enhance the aqueous solubility of hydrophobic odorants, but their exact functions in olfaction remain uncertain [15, 16]. There are evidences that olfactory receptors work also as mechanoreceptors: odorant receptors (ORs), a large family of G protein-coupled receptors, underline the responses to both chemical and mechanical stimuli in mouse olfactory sensory neurons (OSNs) [17, 18, 19]. The study of Timothy Connelly et al [18] reveals an unidentified cascade for mechanotransduction in neurons and suggests that G protein-coupled receptors may have an overlooked function as mechanical sensors. This finding establishes a molecular mechanism through which the nose sends an afferent signal of breathing to the brain to facilitate integration of orofacial sensation and synchronize delta/theta-band activity in certain brain regions with respiration.

The activation of olfactory GPCRs transduces extracellular odorant signals into an intracellular signal by activating the heterotrimeric G_{olf} protein [20, 21, 22, 23], which possesses intrinsic GTPase activity. In its basal state, G proteins exist as heterotrimers composed by three distinct subunits, α, β, and γ. When an odorant molecule binds to and activates the GPCR, the resulting change in the receptor conformation leads to a conformational change in the G protein, which results in the dissociation of GDP from the α subunit and the subsequent binding of GTP. Inactivation of the G protein occurs when the bound GTP is hydrolyzed to GDP, a process that can be accelerated by regulators of G proteins or GTPase-activating proteins [24, 25]. Another class of proteins, the guanosine nucleotide exchange factors (GEFs), enhances the G protein signaling by catalyzing the dissociation of GDP. The protein Ric-8B is a putative GEF expressed in OSNs [20, 26, 27, 28]. Stimulus binding leads to increase intraciliary cyclic adenosine monophosphate (cAMP) levels via sequential activation of olfactory G protein(G_{olf}) and type III adenylyl cyclase (ACIII) [29, 30, 31, 32]. Similar to the channels in the retinal rod outer segment membranes, the increase in the intracellular cAMP concentration ([cAMP]) in the olfactory cilia causes cyclic nucleotide gated (CNG) channels to open, allowing hundreds of thousands of ions to enter the cell, including the concentration of calcium ions ($[Ca^{2+}]$), and the depolarization of the ciliary membrane [33, 34, 35]. As with the retinal system, the rise of the intracellular $[Ca^{2+}]$ opens the Ca^{2+}-activated chloride (CAC) channels and promotes the efflux of chloride anions (Cl^-) from the cilia to the outside of the cell, which amplifies the depolarization initiated by the opening of CNG channels [36, 37, 38, 39, 40]. The amplitude of this depolarization depends on the nature and amount of the odorant molecules detected by the olfactory receptor. The receptor potential triggers an action potential, which transmits odor information to the brain. Therefore, all the olfactory information sent to the brain is

transmitted through the signaling molecules that couple the olfactory stimulus to ion channels [41].

Calcium ion influx is a key component of the odorant evoked current through olfactory CNG channels. The influx of Ca^{2+} has several important consequences in addition to supplying inward a depolarizing receptor current. Ca^{2+} influx through CNG channels during odorant stimulation also exerts negative feedback onto the CNG channel itself, acting as a brake to retard further activity and regulates the activity of a number of the enzymes involved in the second messenger cascades in olfactory signal transduction. These actions of Ca^{2+} are particularly important for signal adaptation [42, 43].

Olfactory receptor neuron excitation is terminated by a number of mechanisms. An obvious one is the unbinding and disappearance of the odorant from the chemoreceptive site located at the surface of the cilia, maybe aided by odorant binding protein (OBP).

3. Stimulus-receptor site interaction

The interaction energy between the odorant molecule and the receptor site should be a weak one, i. e., on the order of a few times k_BT, to allow fast disappearance of the first signal when the surrounding atmosphere is changed. Despite this weak interaction, it should produce a large effect because sensitivities of the order of a small number of odorant molecules per receptor cell have been reported at threshold. This large effect must be able to produce an increase in the conductance of a limiting resistance surface of the receptor neuron and in the density of charge carriers to depolarize the whole or limited region of the surface. The number of charge carriers crossing the olfactory receptor neuron must be a large number times the number of adsorbed molecules [44].

4. Static and dynamic sensitivities

The ability to detect and respond in an adaptive manner to chemical signals serves as the primary window to the sensory world for most species of animals. Chemical sensitivity is present even in the simplest of the extant life forms: bacteria, slime molds, and protozoans. Sensitivity is a highly important issue in the development of an effective biosensor, thus enormous efforts have been made to maximize sensitivity in several detection systems.

Physically speaking, the odorant molecules could diffuse passively or directly (static process), or they could be actively transported to the site of OR interaction by way of proteins in the mucus (dynamic process). The main function of OBPs (small soluble dimeric proteins) in olfactory system is to solubilize and transfer hydrophobic odorant into aqueous phase. This function is important in increasing the sensitivity of olfactory receptor because the presence of OBPs increased the signal intensity of Ca^{2+} influx.

Although various studies have been conducted to investigate the functions of OBPs in natural systems, no study has yet examined the effects of OBPs specificity on the sensitivity of olfactory receptor. The competitive mechanisms of odorant-olfactory receptor and odorant-OBP-olfactory receptor interactions were also suggested based on analytical methods using statistical physics formalism through the study of the variation of the static and the dynamic sensitivities according to the concentration of the two muscone enantiomers (ℓ-muscone and d-muscone) on the mouse muscone receptor MOR215-1.

The static sensitivity expresses the single olfactory response per unit odorant molecule concentration which is related to the discrimination threshold which can be defined by the following relation [45, 46]:

$$s = \frac{R_{\sin}}{C} \tag{1}$$

We have developed, in a previous paper [11], six expressions of theoretical adsorption models, based on the grand canonical ensemble in statistical physics, with the purpose of selecting from them an adequate statistical physics model of the single olfactory response of

the two muscone enantiomers (ℓ-muscone and d-muscone) onto the mouse muscone receptor MOR215-1. Their chemical structures are presented in Fig. 1.

The fitting of the experimental curves demonstrated that the proposed adequate model presented a good correlation with the experimental data. It is specified by a ‘‘monolayer adsorption with identical sites model’’ to characterize the musky stimulus–receptor site interaction.

The non-linear form of the monolayer adsorption with identical sites model can be represented as:

$$R_{\sin} = \alpha N_o = \frac{R_M}{1+(\frac{C_{1/2}}{C})^n} \qquad so \qquad s = \frac{R_M}{C[1+(\frac{C_{1/2}}{C})^n]} \tag{2}$$

Where R_M is the saturation response which is related to N_M and α, $C_{1/2}$ is the concentration at half saturation which is related to the adsorption energy, n represents the fraction or the number of adsorbed molecule(s) per site and α is a transduction coefficient. The values of the analytical adjustment coefficient ℓ-muscone and d-muscone alone are 0.99954 and 0.99577, respectively and the fitting physico-chemical parameters are presented in Table 1.

Fig. 2 shows that in the threshold vicinity, stimulus concentration is low, i. e., $C << C_{1/2}$, the olfactory response expressions ($R_{sin} \sim \frac{R_M C^n}{C_{1/2}^{\ n}}$) indicates that the static sensitivity $s \sim \frac{R_M C^{n-1}}{C_{1/2}^{\ n}}$ increases with decreasing n for a given concentration and for any n (Fig. 3). Then, we can conclude that the steric parameter n controls the sensitivity. This trend of sensitivity is inversed for a concentration in the vicinity of $C_{1/2}$. The static sensitivity moves toward high concentrations if the concentration at half saturation $C_{1/2}$ increases. More the concentration at

half saturation of this stimulus is elevated, more the sensitivity decreases. Indeed, more the concentration is great more the olfactory system needs time for adaptation (loss of sensitivity). At half saturation, when concentration C is equal to $C_{1/2}$, the static sensitivity is approximately expressed as a function of the parameters R_M and the inverse of half saturation concentration, $C_{1/2}$ and can be written as: $s \sim \frac{R_M}{C_{1/2}}$. For high concentrations, i. e., $C >> C_{1/2}$, the totality of receptor sites are occupied. Thus the value of the static sensitivity tends towards zero.

The dynamic or differential sensitivity of the mouse muscone receptor MOR215-1 is defined by the following expression [45, 46]:

$$s' = \frac{dR}{dC} \tag{3}$$

Using the analytical expression of the olfactory response with the monolayer adsorption model with identical sites, the sensitivity takes the form:

$$s' = nR_M C_{1/2}{}^n \frac{C^{-(n+1)}}{[1+(\frac{C_{1/2}}{C})^n]^2} \tag{4}$$

The variation of the dynamic sensitivity s' according to the concentration of the two muscone enantiomers (ℓ-muscone and d-muscone) on the mouse muscone receptor MOR215-1, which has some differences in behavior from the static sensitivity s, is represented in Fig. 4.

Fig. 4 presents the variation of dynamic sensitivity s' versus the concentrations of the two stimuli. For low concentration relative to $C_{1/2}$, when $C << C_{1/2}$, the dynamic sensitivity of the olfactory membrane is approximately expressed as a function of the parameters n, R_M and the

inverse of the half saturation concentration $C_{1/2}$: s' $\sim \frac{nR_M C^{n-1}}{C_{1/2}{}^n}$. At half saturation, when concentration is equal to $C_{1/2}$, the dynamic sensitivity can be written: s' $\sim \frac{nR_M}{4C_{1/2}}$. However, for high concentrations ($C >> C_{1/2}$), the value of dynamic sensitivity tends towards zero as for the static sensitivity which can be explained by the fact that the totality of receptor sites becomes occupied.

5. Structure-activity relationship: Receptor site size distribution (RSD)

The link between the molecular structure of an odorant and its perceived odor quality was pointed out by Linus Pauling only in the middle of the twentieth century [47]. Nevertheless, the notion of structure–odor relationships was first applied to odorant molecules by Amoore [48, 49], who established a list of primary odors. Furthermore, the development of computational tools led to the appearance of quantitative structure–activity relationships, which attempts to correlate an experimental response (biological activity or a physico-chemical property) with some molecular properties.

The odorant molecule can produce the conformational changes of olfactory receptor site. Such structure would not allow the entrance of a large molecule into the binding cavity without a major conformational change [50, 51]. Proteins are not rigid bodies and can change shape. The molecular volume of an odorant molecule should match the dimensions of the receptor site. Subsequently, the odorant molecule can fit into the binding site of the OR and trigger signal transduction. Indeed, the interactions between odorant molecule and receptor site have a prominent impact on charges distribution of the receptor. The odor bound binding proteins (receptor site) activate second messengers (e.g. G-proteins). The activated second messengers cause a change in the conductivity of ion channels. Through ionic influx a depolarization can

build an action potential. Furthermore, the amount of change in the membrane potential of an olfactory receptor neuron depends on the number of activated olfactory receptor sites and the time that they remain activated, which are determined by various physico-chemical properties of the ligand (odorant) and the receptor, but here we focus only on the size of the receptor site or the binding-pocket.

We could know the size of the receptor site, if we knew its three dimensional structure. But this is not the case ongoing here; it is not easy to know the structure of integral proteins, including olfactory receptor. Thus, the topic of this part of ongoing researches is determining the receptor site size distribution (RSD), through the use of the grand canonical ensemble in statistical physics and the Kelvin equation and to study the influence of the steric interaction between the odorant molecules and receptor sites.

In this study we suggest that the surface of the mouse muscone receptor MOR-215-1 is porous and the musky odor is accounted for by molecules with the shape of a disk about 1 nanometer in diameter (0.5 nm in radius) [49]. This meant that the receptor site for musky molecules must be a disk about minimum one nanometer in diameter.

The vapor pressure P of the odor molecule in receptor site of radius r (in nm) is given by the following Kelvin equation [52]:

$$\ln\left(\frac{P}{P_0}\right) = -\frac{2\gamma V_L}{rRT}\cos\theta \tag{5}$$

Where P_0 is the saturation vapor pressure of the adsorbate, γ is its surface tension, V_L is the molar volume of the liquid adsorbate, R is the ideal gas constant (8.3143 10^{18} J.nm^2 (K.mol.m^2)$^{-1}$), T is the absolute temperature and θ is the contact angle. From Kelvin equation Eq. 5, we can deduce:

$$\frac{P}{P_0} = e^{-\frac{2\gamma V_L}{RT}\frac{1}{r}} = e^{-\frac{C_k}{r}} \tag{6}$$

Where C_k is the Kelvin constant.

In the case of muscone enantiomers, the corresponding parameters at 298 K that we have used [53] are illustrated in Table 2. We have used θ =0°.

The realized model can also be applied to liquid phase adsorption systems by replacing $\frac{P}{P_0}$ with $\frac{C}{C_s}$ [54]. The derivative of the single olfactory response relative to receptor radius gives the receptor site size distribution expression [55]:

$$RSD = \frac{dR_{\sin}}{dr} \tag{7}$$

$$\frac{dR_{\sin}}{dr} = \frac{d}{dr}\left[\frac{R_M}{1+\left(e^{-\frac{\Delta E^a}{RT}} e^{\frac{C_k}{r}}\right)^n}\right] = \frac{nR_M C_k \left(e^{-\frac{\Delta E^a}{RT}} e^{\frac{C_k}{r}}\right)^n}{r^2\left[1+\left(e^{-\frac{\Delta E^a}{RT}} e^{\frac{C_k}{r}}\right)^n\right]^2} \tag{8}$$

According to the two muscone enantiomers responses, the receptor site size distributions of the mouse muscone receptor 215-1 sites were determined, as presented in Fig. 5. It can be seen that the mouse muscone receptor 215-1 possesses a multiple site distribution ranging from microreceptors to mesoreceptors size. The receptor site size distribution of each olfactory sensory neuron may be determined by introducing the Kelvin equation in the expression of the statistical physics model. It depends on several parameters such as the fraction or number of molecule(s) per site n, the response at saturation R_M and the Kelvin constant C_k. Through our model based on the statistical physics, we can deduce that ℓ-muscone molecules occupy smaller receptor sites than d-muscone (Fig. 5). The Fig.5 shows receptor site size distributions with peaks at around 4 nm for ℓ-muscone and at around 6 nm for d-muscone.

6. Olfactory band

Odorants are bound to the receptor sites with the same adsorption energy (-ε) that gives the molar adsorption energy from dissolved state ΔE^a. By using the single energy expression for all receptor sites, we can easily interpret the adsorption results because in the case of multi-energy model, the statistical treatment would be more difficult and also the model expression would be more complicated. The molar adsorption energy, ΔE^a, can be represented by the depth of potential well which exist on receptor sites of the mouse odorant receptor neuron MOR215-1.

The values of the molar adsorption energies of dissolved molecules ΔE^a for each muscone enantiomer molecule (for ℓ-muscone is 15.868 kJ/mol and for d-muscone is 4.202 kJ/mol), using the fitted energetic physico-chemical parameters $C_{1/2}$(for ℓ-muscone is 1.53 10^{-6} mol/L and for d-muscone is 1.70 10^{-4} mol/L) calculated in our previous work [11] showed that the two muscone enantiomers ℓ-muscone and d-muscone are binding onto the mouse muscone receptor MOR215-1 with a physical adsorption, since the values of the adsorption energies do not exceed 40 kJ/mol. This is a direct method to give the proof that the stimuli keep their chemical structure after the adsorption process at the receptor site. For equal values of solubility, $C_{1/2}$ decreases as adsorption energy increases. Therefore, the low value of $C_{1/2}$, corresponding to the large value of adsorption energy, involving strong odorant-receptor site interaction and the adsorption is improved. Thus, we can deduce that the receptor sites that have the stronger energy will be rapidly and easily occupied by odorant molecules, whereas, for large value of $C_{1/2}$, which correspond to low energy value, i.e., a low binding energy and the adsorption is reduced.

This physical adsorption is achieved through “weak” intermolecular forces like Van der Waals or hydrogen binding [56, 57] that play a significant role in a great variety of physical, chemical and biological phenomena.

IUPAC has recently proposed the following definition [58]: The hydrogen bond is an attractive interaction between a group X-H and an atom or group of atoms Y in the same or different molecule(s). Although a normal hydrogen bond X-H…Y is weak compared to covalent bonds, it is generally strong enough to keep two molecules together. X [59] may be any element having electronegativity greater than of H (F, N, O, C, P, S, Cl, Se, Br and I) and Y [60] could be any of these elements. Also, H atom itself can form a hydorgen bond as acceptor and it was called dihydrogen bonding [61]. Pauling has suggested a range from 8 to 42 kJ/mol as a typical bond [62] that does not cover the bifluoride anion $(FHF)^-$. For exemple, O – H …N: 29 kJ/mol; O – H …O: 21 kJ/mol; N – H …N: 13 kJ/mol; N – H …O: 8 kJ/mol; HO – H …OH_3^+: 18 kJ/mol. It is possible for a hydrogen bond to form through the π-electron system of a molecule [63] or simple unsaturated hydrocarbons to form π hydrogen bonds. The binding energies of the lone pair and π complexes are 8.2 and 18.9 kJ/mol, respectively.

Van der Waals are weak attraction between molecules in close proximity to each other. Furthermore, energies associated with Van der Waals interaction are quite small. Usually, they are between 2 and 4 kJ/mol.

The led reasonning about the adsorption process with statistical physics formalism allows to introduce all the energies of the odrant molecule. The translation energy is the only necessary form to perform adsorption.Without it we can not speak of any adsorption phenomenon. All the other energies come from the internal degrees of the molecule as rotational, vibrational, electronic, … etc, which constitute different forms of exchange of energy between the odorant molecules themselves and between stimulus and olfactory receptor. There are many reasons to eliminate the major part of internal degrees of energies like rotational, electronic and nuclear

except the vibrational. Nuclear and electronic energy levels are enough high to be not sufficiently excited at ambient temperature. Rotational degree could be in principale activated at the ambient temperature, however the mucus solution and the size of the muscone molecules constitute a hindrance to the rotation of the molecule [64]. The vibration degree is the only contribution which could not be eliminated. In addition, it is known that some authors suggested that vibrational energy of odorant molecule is a principal vector of the olfactory signal. Thus, with the use of the fitting model we are able to investigate quantitatively and qualitatively the intervention of the vibrational energy in the olfactory mechanism by calculating its proportion in that mechanism, which we did not here. Therefore, we can say that each receptor responds to a particlular frequency stimulation when odorant molecules bind to all the receptor sites necessary to complete the transduction of olfactory signal, then the odor is perceived. Thus, we can say that the infrared spectrocopy is a powerful tool for determing the olfactory band. Intermolecular vibration provides information on the interaction of the atom or group with other parts of the receptor site. In this part, we study the physico-chemical nature of membrane receptor site behavior by investigating the typical molecular vibration of the mouse receptor using statistical physics reatment.

There are two types of vibrational theories of odor. One type suggests that the effective stimulus is intramolecular vibration of the odorant molecules which is detected by the sensory nerves. Proponents of this view were: Ungerer, Dyson, Teudt, Turin and Wright. For example, the theory of wright [65], that has its origins in the view of Dyson [66], suggested the odors of chemicals are associated with their intramolecular vibrational frequencies in the far infrared region of the electromagnetic spectrum. The only difference between them is that Dyson directed attend to the frequency range of 1500-3000 cm^{-1}, while Wright had concentered on the lower frequency range of 100-700 cm^{-1}. Moreover, at the late 1990s, the vibrational theory was developed by the introduction of a new biological transduction mechanism of molecular

vibrations based on the concept of inelastic electron tunneling [67]. The other type considers that the odor stimulus is transported at long range from the source of the nose by a propagated electromagnetic radiation, may be ultraviolet, but more often infrared. Supporters of this concept include Ogle, Fabre, Hyninx, Beck and Callahan [68].

We use the infrared spectroscopy to study the vibrational interaction between odorant molecules and receptor sites. According to Turin [67], volatile molecule can get specific sensations of their vibrational mode, which can excite the receptor bonds in the frequency regions associated with a particular fragrance. This means that the surface of the olfactory receptor (may be pigment) absorbs vibrations of odor affecting the continuous cells in which the olfactory nerves end.

As we have previously shown that the exchanged energy between an odorant and olfactory receptor to manifest a perception is an electromagnetic radiation in the infrared range. Then, it is the same type as that for vision that has two excitation mechanisms: optical and thermal excitation [69]. Moreover, we can remove the optical one because on the one hand, the energy of photon in the visible and infrared domain is largely different and on the other hand, the perception of odorant exist regardless of whether the substance is lit or not. At the end, only the thermal energy kept which cannot be eliminated in the olfactory mechanism. Indeed, the major characteristics of the microscopic mechanism of smell are temperature dependent and that odor is only a particular form of thermal energy which is the adsorption energy. So we can determine after this study the olfactory band that is most probably between 2 and 42 kJ/mol corresponding to the infrared range: 200 - 3500 cm^{-1}.

7. Conclusions

In this paper, we conclude that olfactory transduction covers all the biochemical (production of second messengers) and electrical (opening of ionic channels) steps from odorant molecule binding on the olfactory receptor site until the emission of action potentials by the olfactory sensory neuron.

Olfactory systems have evolved great discriminatory power and extraordinary sensitivity whose expression is established through the use of the grand canonical ensemble in statistical physics and the applying of some assumptions and the present results demonstrate that the mouse muscone receptor MOR215-1 is much more sensitive to ℓ-muscone than to d-muscone. Further, the high sensitivity of the olfactory receptor cell is a consequence of signal amplification mechanisms.

In olfaction process; it is generally believed that microreceptors are the major provider of binding sites, whereas, in mesoreceptors only weaker adsorption is observed [70], which maybe lead to a weak perceived response (d-muscone).

In conclusion, by means of our statistical physics investigation we have determined the interval energy which is approximately between 2 and 42 kJ/mol corresponding to the infrared range: 200- 3500 cm^{-1} that we can name it olfactory band.

References

[1]Hecht, S., Shlaer, S., & Pirenne, M. P. (1942). Energy, quanta and vision. General Physiology, 25, 819–840.

[2]Liebman, P. A., & Pugh, E. N. (1979). The control of phosphodiesterase in rod disk membranes: kinetics, possible mechanisms and significance for vision. Vision Research, 19, 375–380.

[3]Pappone, M. C., Hurley, J. B., Bourne, H. R., & Stryer, L. (1982). Functional homology

between signal coupling proteins. Cholera toxin inactivates the GTPase activity of transducin. Biological Chemistry, 257, 10540–10543.

[4]Fung, B. K., Hurley, J. B., & Stryer, L. (1981). Flow of information in the light-triggered cyclic nucleotide cascade of vision. Proceedings of the National Academy of Sciences of the United States of America, 78, 152–156.

[5]Apfelbach, R., Parsons, M.H., Soini, H. A., & Novotny, M. V. (2015). Are single odorous components of a predator sufficient to elicit defensive behaviors in prey species?. Frontiers in Neuroscience, 9, article 263.

[6]Breer, H., Boekhoff, I., & Tareilus, E. (1990). Rapid kinetics of second messenger formation in olfactory transduction. Nature, 345, 65–68.

[7]Bargmann, C. I. (2006). Comparative chemosensation from receptors to ecology. Nature, 444, 295-301.

[8]Ohloff, G. (1994). Scent and fragrances: the fascination of odors and their chemical Perspectives. NY: Springer.

[9]Keyhani, K., Sherer, P. W., & Mozell, M. M. (1996). A Numerical Model of Nasal Odorant Transport for the Analysis of Human Olfaction. Theoretical Biology, 186, 279-301.

[10]Shirasu, M., Yoshikawa, K., Takai, Y., Nakasima, A., Takeuchi, H., & Sakano, H. (2014). Olfactory receptor and neural pathway responsible for highly selective sensing of musk odors. Neuron, 81, 165-178.

[11]Ben Khemis, I., Mechi, N., Sellaoui, L., & Ben Lamine, A. (2016). Modeling of muscone enantiomers olfactory response by an adsorption process onto the mouse muscone receptor MOR215-1. Journal of Molecular Liquids, 221, 896-903.

[12]Ben Khemis, I., Mechi, N., & Ben Lamine, A. (2016). Olfactory response modeling of mouse muscone receptor MOR215-1 to binary muscone enantiomers odor by statistical physics models. Journal of Molecular Liquids, 224, 562-570.

[13]Menco, B. P. (1997). Ultrastructural aspects of olfactory signaling. Chemical Senses, 22, 295-311.

[14]Schild, D., & Restrepo, D. (1998). Transduction mechanisms in vertebrate olfactory receptor cells. Physiological Reviews, 78, 429-466.

[15]Mastrogiacomo, R., D Ambrosio, C., Niccolini, A., Serra, A., Gazzano, A., Scaloni, A., et al. (2014). An odorant-binding protein is abundantly expressed in the nose and in the seminal fluid of the rabbit. PLoS One, 9, e111932.

[16]Tegoni, M., Pelosi, P., Vincent, F., Spinelli, S., Campanacci, V., Grolli, S., et al. (2000). Mammalian odorant binding proteins. Biochimica et Biophysica Acta, 1482, 229-240.

[17]Chen, X., Xia, Z., & Storm, D. R. (2012). Stimulation of electro-olfactogram responses in the main olfactory epithelia by airflow depends on the type 3 adenylyl cyclase. Neuroscience, 32, 15769-15778.

[18]Connelly, T., Yu, Y., Grosmaitre, X., Wang, J., Santarelli, L. C., Savigner, A., et al. (2015). Gprotein-coupled odorant receptors underlie mechanosensitivity in mammalian olfactory sensory neurons. Proceedings of the National Academy of Sciences of the United States of America, 112, 590-595

[19]Grosmaitre, X., Santarelli, L. C., Tan, J., Luo, M., & Ma, M. (2007). Dual functions of mammalian olfactory sensory neurons as odor detectors and mechanical sensors. Nature Neuroscience, 10, 348-354.

[20]Chan, P., Gabay, M., Wright, F. A., Kan, W., Oner, S. S., Lanier, S. M., et al. (2011). Purification of heterotrimeric G protein alpha subunits by GST-Ric-8 association: primary characterization of purified G alpha(olf). Biological Chemistry, 286, 2625-2635.

[21]Jones, D. T., Masters, S. B., Bourne, H. R., & Reed, R. R. (1990). Biochemical characterization of three stimulatory GTP-binding proteins. The large and small forms of Gs and the olfactory-specific G-protein, Golf. Journal of Biological Chemistry, 265, 2671-2676.

[22]Jones, D. T., & Reed, R. R. (1989). Golf: an olfactory neuron specific-G protein involved in odorant signal transduction. Science, 244, 790-795.

[23]Schandar, M., Laugwitz, K. L., Boekhoff, I., Kroner, C., Gudermann, T., Schultz, G., et al. (1998). Odorants selectively activate distinct G protein subtypes in olfactory cilia. Biological Chemistry, 273, 16669-16677.

[24]Bruch, R. C., & Medler, K. F. (1996). A regulator of G-protein signaling in olfactory receptorneurons. NeuroReport, 7, 2941-2944.

[25]Norlin, E. M., & Berghard, A. (2001). Spatially restricted expression of regulators of G-protein signaling in primary olfactory neurons. Molecular and Cellular Neuroscience, 17, 872-882.

[26]Kerr, D. S., Von Dannecker, L. E., Davalos, M., Michaloski, J. S., & Malnic, B. (2008). Ric-8B interacts with G alpha olf and G gamma 13 and co-localizes with G alpha olf, G beta 1 and G gamma 13 in the cilia of olfactory sensory neurons. Molecular and Cellular Neuroscience, 38, 341-348.

[27]Von Dannecker, L. E., Mercadante, A. F., &Malnic, B. (2005). Ric-8B, an olfactory putativeGTP exchange factor, amplifies signal transduction through the olfactory-specific G-protein Galphaolf. Neuroscience, 25, 3793-3800.

[28]Von Dannecker, L. E., Mercadante, A. F., & Malnic, B. (2006). Ric-8B promotes functional expression of odorant receptors. Proceedings of the National Academy of Sciences of the United States of America, 103, 9310-9314.

[29]Bakalyar, H. A., & Reed, R. R. (1990). Identification of a specialized adenylyl cyclase that may mediate odorant detection. Science, 250, 1403-1406.

[30]Lowe, G., Nakamura, T., & Gold, G. H. (1989). Adenylatecyclase mediates olfactory transduction for a wide variety of odorants. Proceedings of the National Academy of Sciences of the United States of America, 86, 5641-5645.

[31]Wayman, G. A., Impey, S., & Storm, D. R. (1995). Ca^{2+} inhibition of type III adenylyl cyclase in vivo. Biological Chemistry, 270, 21480-21486.

[32]Wong, S. T., Trinh, K., Hacker, B., Chan, G. C., Lowe, G., Gaggar, A., et al. (2000). Disruptionof the type III adenylyl cyclase gene leads to peripheral and behavioral anosmia in transgenicmice. Neuron, 27, 487-497.

[33]Kaupp, U. B., & Seifert, R. (2002). Cyclic nucleotide-gated ion channels. Physiological Reviews, 82, 769-824.

[34]Kleene, S. J. (2008). The electrochemical basis of odor transduction in vertebrate olfactory cilia. Chemical Senses, 33, 839-859.

[35]Nakamura, T., & Gold, G. H. (1987). A cyclic nucleotide-gated conductance in olfactory receptor cilia. Nature, 325, 442-444.

[36]Kleene, S. J. (1997). High-gain, low-noise amplification in olfactory transduction. Biophysical, 73, 1110-1117.

[37]Kurahashi, T., &Yau, K. W. (1994). Olfactory transduction. Tale of an unusual chloride current. Current Biology, 4, 256-258.

[38]Reisert, J., Bauer, P. J., Yau, K. W., &Frings, S. (2003). The Ca-activated Cl channel and itscontrol in rat olfactory receptor neurons. General Physiology, 122, 349-363.

[39]Stephan, A. B., Shum, E. Y., Hirsh, S., Cygnar, K. D., Reisert, J., & Zhao, H. (2009). ANO2 is the cilial calcium-activated chloride channel that may mediate olfactory amplification. Proceedings of the National Academy of Sciences of the United States of America, 106, 11776-11781.

[40]Takeuchi, H., & Kurahashi, T. (2005). Mechanism of signal amplification in the olfactory sensory cilia. Neuroscience, 25, 11084-11091.

[41]Torre, V., Ashmore, J. F., Lamb, T. D., & Menini, A. (1995). Transduction and adaptation in sensory receptor cells. Neuroscience, 15, 7757-7768.

[42]Chen, T. Y., &Yau, K. W. (1994). Direct modulation by Ca^{2+}-calmodulin of cyclic nucleotide-activated channel of rat olfactory receptor neurons. Nature, 368, 545-548.

[43]Kurahashi, T., & Menini, A. (1997). Mechanism of odorant adaptation in the olfactory receptor cell. Nature, 385, 725-729.

[44]Rosenberg, B., Mirsa, T. N., & Switzer, R. (1968). Mechanism of olfactory transduction. Nature, 217, 423-427.

[45]Knani, S., Khalfaoui, M., Hchicha, M. A., Mathlouthi, M., & Ben Lamine, A. (2014). Interpretation of psychophysics response curves using statistical physics. Food Chemistry, 151, 487-499.

[46]Ben Lamine, A., & Bouazra, Y. (1997). Application of statistical thermodynamics to the olfaction mechanism. Chemical Senses, 22, 67-75.

[47]Pauling, L. (1946). Molecular architecture and biological reactions. Chemical Engineering News, 24, 1365–1377.

[48]Amoore, J. E. (1952). The stereochemical specificities of human olfactory receptors. Perfumery and Essential Oils Records. 43, 321–330.

[49]Amoore, J. E. (1963). Stereochemical theory of olfaction. Nature, 198, 271–272.

[50]Pelosi, P., Calvello, M., & Ban, L. (2005). Diversity of odorant-binding proteins and chemosensory proteins in insects. Chemical Senses, 30, 291–292.

[51]Lescop, E., Briand, L.,Pernollet, J.C., & Guittet, E.(2009). Structural basis of the broad specificity of a general odorant-binding protein from honeybee. Biochemistry, 48, 2431–2441.

[52]Huang, B., Bartholomew, C. H., & Woodfield, B. F. (2014). Improved calculations of pore size distribution for relatively large, irregular slit-shaped mesopore structure. Microporous and Mesoporous Materials, 184, 112-121.

[53]http://www.chemspider.com.

[54]Khalfaoui, M., Knani, S., Hachicha, M.A., & Ben Lamine, A. (2003). New theoretical expressions for the five adsorption type isotherms classified by BET based on statistical physics treatment. Colloid and Interface Science, 263, 350-356.

[55]Aouaini, F., Knani, S., Ben Yahia, M., Bahloul, N., Ben Lmaine, A., & Kechaou, N. (2015). Investigation of pore size and energy distributions by statistical physics formalism applied to agriculture products. Physica A, 439, 150-159.

[56]Sellaoui, L,. Guedidi, H., Masson, S., Reinert, L., Levêque, J. M., Knani, S., Ben Lamine, A., Khalfaoui, M., & Duclaux, L. (2016). Steric and energetic interpretations of the equilibrium adsorption of two new pyridinium ionic liquids and ibuprofen on a microporous activated carbon cloth: statistical and COSMO-RS models. Fluid phase equilibria, 414, 156-163.

[57]Ertl, G. (1989). Thermodynamics of gas-surface interactions. Pure and Applied Chemistry, 61, 1001-1007.

[58]Arunan, E. (2007). Hydrogen bonding and other molecular interactions. Current Science, 92, 17-18.

[59]Kollman, P. A., & Allen, L. C. (1972). Theory of the hydrogen bond. Chemical Reviews, 72, 283-303.

[60]Kryachko, E. S., Karpfen, A., & Remacle, F. (2005). Nonconventional hydrogen bonding between clusters of gold and hydrogen fluoride. Physical Chemistry A, 109, 7309-7318.

[61]Crabtree, R. H., Siegbahn, P. E. M., Eisenstein, O., Rheingold, A. L., & Koetzle, T. (1996). A new intermolecular interaction: unconventional hydrogen bonds with element-hybride bonds as proton acceptor. Accounts of Chemical Research, 29, 348-354.

[62]Pauling, L. (1931). The nature of the chemical bond. Application of result obtained from the quantum mechanics and from a theory of paramagnetic susceptibility of the structure of molecules. Journal of the American Chemical Society, 53, 1367-1400.

[63]Gotch, A.J., & Zwier, T. S. J. (1992). Multiphotonionization studies of clusters of immiscible liquids: 1. C6H6-(H2O)n, n=1,2. Chemical Physics, 96, 3388-3401.

[64]Herzberg, G. (1950). Molecular spectra and molecular structure, Van Nostrand Reinhold Company, 1, 464-482.

[65]Wright, R. H. (1957). Molecular structure and organokptic quality. S.C.I. Monograph, 1, 91-102.

[66]Dyson, G. M. (1938). The scientific basis of odour. Chemistry and Industry, 57, 647-651.

[67]Turin, L. (1996). A spectroscopic mechanism for primary olfactory reception. Chemical Senses, 21, 773-791.

[68] Dan Mckenzie, M. D. (1923). Aromatic and the Soul (A study of Smells). London WILLIAM HEINEMANN (MEDICAL BOOKS) LTD.

[69] Yue, L., Weiland, J. D., Roska, B., & Humayun, M. S. (2016). Retinal stimulation strategies to restore vision: Fundamentals and systems. Progress in Retinal and Eye Research, 53, 21-47.

[70]Wu, C. H., Shr, J. F., Wu, C. F., & Hseih, C. T. (2008). Adsorption energy distribution of carbon tetrachloride on carbon nanofiber arrays prepared by template synthesis. Physica E, 40, 814-821.

Table 1 Adjustment parameters values corresponding to the monolayer model with identical sites (or Hill model).

Parameters	**ℓ-muscone**	**d-muscone**
R_M (a.u)	1.05 ± 0.01	1.03 ± 0.03
n	1.89 ± 0.07	2.44 ± 0.24
$C_{1/2}$ (mol/L)	$1.53\ 10^{-6} \pm 4.08\ 10^{-8}$	$1.70\ 10^{-4} \pm 1.08\ 10^{-5}$

Table 2 Muscone parameters (ℓ-muscone and d-muscone).

Parameters	**ℓ or d-muscone**
γ (N/m)	$27.1\ 10^{-3}$
V(m^3/mol)	$282.6\ 10^{-6}$
C_k (nm)	6.18

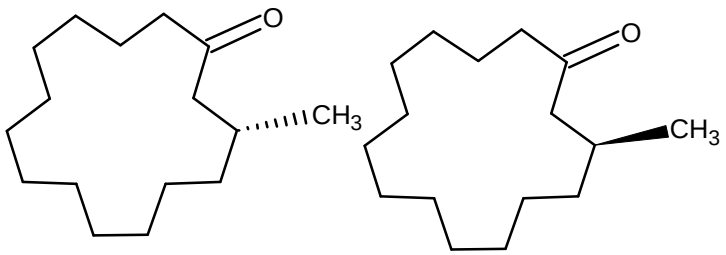

l-muscone d-muscone

Fig. 1 chemical structures of ℓ-muscone and d-muscone; molecular formula: $C_{16}H_{30}O$ and chemical name: 3-Methylcyclopentadecanone.

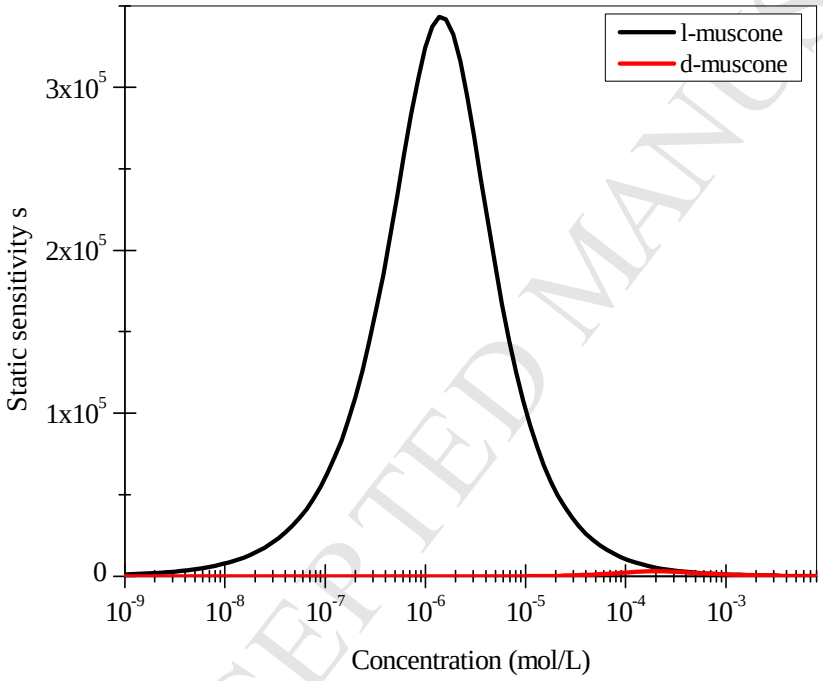

Fig. 2 Evolution of the static sensitivity s according to the concentration of ℓ-muscone and d-muscone separately on the mouse muscone receptor MOR215-1.

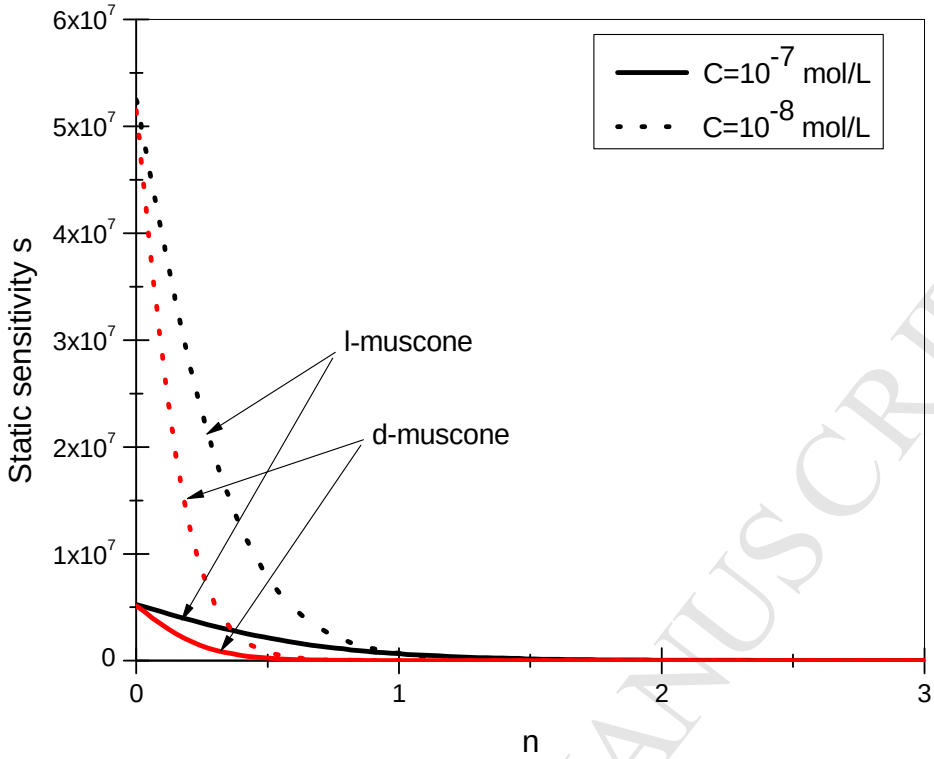

Fig. 3 Evolution of the static sensitivity s according to the number of molecules per site of ℓ-muscone and d-muscone on the mouse muscone receptor MOR215-1.

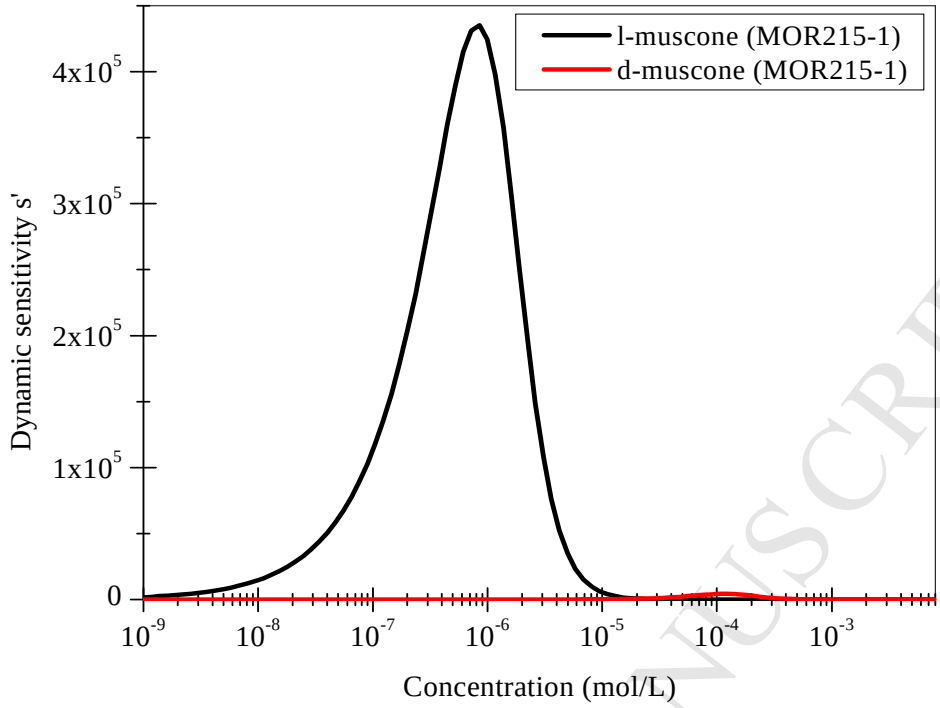

Fig. 4 Evolution of the dynamic sensitivity s' according to the concentration of ℓ-muscone and d-muscone on the mouse muscone receptor MOR215-1.

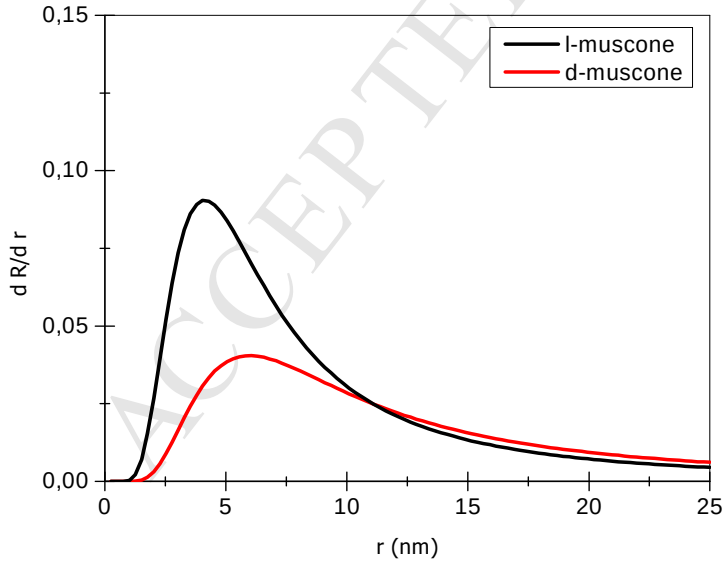

Fig. 5 The RSD of musky receptor sites with, R_M = 1.05 (a. u) and n= 1.89 (ℓ-muscone), R_M = 1.03 (a. u) and n= 2.44 (d-muscone).

Highlights

-static and dynamic sensitivities were developed in this work according to the monolayer model with identical sites.

- Receptor site size distribution was calculated according to the monolayer model with identical sites.

- Olfactory band was determined through the statistical physics treatment.